Reports of Practical Oncology and Radiotherapy 25 (2020) 515–520

Available online at www.sciencedirect.com

Reports of Practical Oncology and Radiotherapy

journal homepage: http://www.elsevier.com/locate/rpor

Original research article

Enhanced dose measurement of zinc oxide nanoparticles by radiochromic polymer dosimeter and Monte Carlo simulation

Nooshin Banaee *

Department of Medical Radiation, Engineering Faculty, Central Tehran Branch, Islamic Azad University, Tehran, Iran

ARTICLE INFO

Article history:
Received 28 January 2020
Received in revised form 11 March 2020
Accepted 10 April 2020
Available online 27 April 2020

Keywords:
Nano particles
ZnO
Dosimetry
Radiation
Monte carlo.

ABSTRACT

Aim: The aim of this study is to evaluate the effects of Zinc Oxide nanoparticles on dose enhancement factor using PRESAGE dosimeter and Monte Carlo simulation.
Background: High Z materials absorb X-ray remarkably. Among Nano-science, Zinc Oxide nanoparticles are interesting semiconductors, producing reactive oxygen species when irradiated by photons. Therefore, it seems that dose enhancement originating by incorporating ZnO NPs in irradiated volume would increase the therapeutic ratio.
Materials and methods: Initially, the PRESAGE dosimeter was fabricated and calibrated. Then Zinc Oxide nanoparticles with an average particle size of about 40 nm were synthesized. At next step, various concentrations of the nanoparticles were incorporated into the PRESAGE composition and irradiated in radiation fields. Then, the mentioned processes were simulated.
Results: Practical measurements revealed that by incorporating 500, 1000 and 3000 $\mu g\,ml^{-1}$ ZnO NPs into PRESAGE the dose enhancement factor of 1.36, 1.39, 1.44 for $1 \times 1\,cm^2$ field size, 1.39, 1.41, 1.46 for $2 \times 2\,cm^2$ and 1.40, 1.45 and 1.50 for $3 \times 3\,cm^2$ could be found, respectively. Simulation results showed that in the mentioned condition, the dose enhancement factor of 1.05, 1.08, 1.10 for $1 \times 1\,cm^2$ field size, 1.06, 1.09, 1.10 for $2 \times 2\,cm^2$ and 1.08, 1.11 and 1.13 for $3 \times 3\,cm^2$ could be derived, respectively.
Conclusion: The results of this study showed that dose enhancement increases by increasing concentration of Zinc Oxide nanoparticles. Many reasons such as photoelectric, pair production effects and even Compton scattering can cause dose enhancement for megavoltage beams.

1. Background

Advanced and complex radiation therapy delivery techniques are currently used with the goal of escalating tumor dose and minimizing normal tissues complications. Among these progressive methods, the use of nanotechnology offers some exciting possibilities including the opportunity of destroying cancerous tumors with minimal damage to healthy tissues[1–6]

Among Nano-science, Zinc Oxide nanoparticles (ZnO NPs) are interesting wide band gap semiconductors (3.37 eV), producing reactive oxygen species (ROS) and oxygen free radicals when irradiated by photons.[7–9] It has been demonstrated that high Z materials absorb X-ray remarkably. Therefore, it seems that dose enhancement originating by incorporating ZnO NPs in irradiated volume would increase the therapeutic ratio significantly.[10–12]

Dose enhancement factor is more important in small radiation fields where the lack of lateral electronic equilibrium condition leads to employing higher numbers of monitor units (MU) to deliver a certain amount of absorbed dose.[12]

It seems that using the recently introduced water equivalent radiochromic PRESAGE dosimeter would be a proper method to evaluate the effects of ZnO NPs. This type of dosimeter is formulated with a free radical initiator, leuco dye and polyurethane and their optical properties are changed in proportion to the absorbed dose.[13]

Another useful method for evaluating dose enhancement is using Monte Carlo (MC) simulation. Several MC studies have been done to explain events responsible for the biological outcomes.[14–15]

2. Aim

The aim of this study is to determine the dose enhancement factor of ZnO NPs by use of the PRESAGE dosimeter and Monte Carlo simulation in small radiation fields.

* Corresponding author.
E-mail address: nooshin_banaee@yahoo.com

https://doi.org/10.1016/j.rpor.2020.04.008
1507-1367/

Table 1
Percentage chemical composition of PRESAGE.

Components	Polyurethane	LMG	CCl4
Percentage (%)	94	1	5

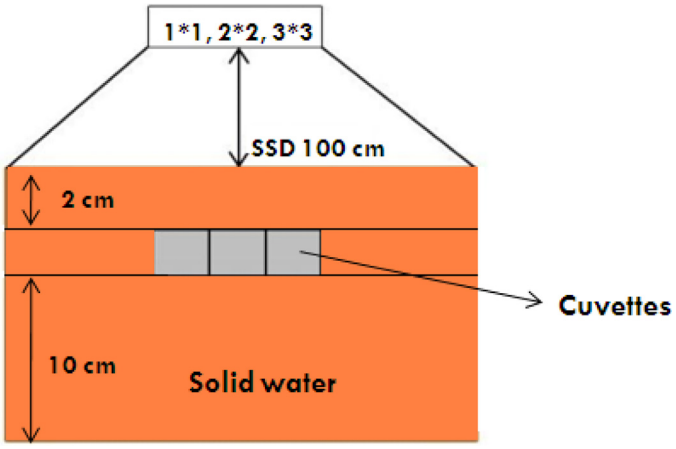

Fig. 1. Set up of irradiation: Various slab phantoms are used to prepare electronic equilibrium condition. The center of PRESAGE filled cuvettes are placed at depth of 2.5 cm.

3. Materials and methods

This study consists of two sections: experimental measurements and Monte Carlo simulations.

3.1. Experimental phase

3.1.1. PRESAGE dosimetry

In order to perform the experimental phase of the study, the water equivalent PRESAGE dosimeter was fabricated. The procedure consists of mixing CCl4 (Merck, Keinlworth, United States) and leucomalachite green (LMG) (Sigma Aldrich, St Louis, MO, United States). Then a polyurethane resin (Crystal Clear 2006, Smooth-On, Easton, PA, USA) which was supplied in two parts (Part A and Part B) were mixed together by ratio of 100 to 90 to afford optically clear polyurethane resins that form the matrix of the PRESAGE dosimeter. The solutions prepared were combined together and thoroughly mixed. Then the prepared mixture was poured into poly spectrophotometer cuvettes and the filled cuvettes were kept in a pressure pot (60 psi) for 5 days to minimize outgassing.[13],[15]

Table 1 shows the percentage composition of PRESAGE. By using mayneord formula and considering the elemental compositions of PRESAGE, the effective atomic number of the fabricated dosimeter would be 7.8.[16]

The maximum pre-irradiation absorptions of cuvettes were then determined using UV-Vis spectrophotometer (Varian, Palo Alto, California, USA). The next process was calibration of PRESAGE against the ionization chamber (Farmer chamber, 0.6 cc, PTW, Freiburg, Germany) to deliver definite steps of absorbed dose. Cuvettes were placed in a solid water phantom made by Plexiglas and irradiated in a $15 \times 15 cm^2$ field to deliver the absorbed doses including 0, 0.5, 1, 2, 4, 6, 8, 10, 12, 14, 16, 18, 20 Gy at depth of 2.5 cm, irradiated by 6 MV photon beams produced by Varian Clinac 2100 C linear accelerator (Varian, Palo Alto, California, USA). Various slab phantoms were used to prepare the electronic equilibrium condition (Fig. 1). For each dose step, three cuvettes were used. All cuvettes were kept in a dark and cold environment to prevent any accidental absorption change and 48 h after irradiation, again by using UV-Vis spectrophotometer, the maximum absorption of each cuvette was obtained. Finally, a calibration curve, which is the variations of optical density changes against absorbed doses, was plotted.

3.1.2. Nanoparticle synthesization

At the next step, ZnO NPs were prepared and incorporated in to the composition of the PRESAGE and the irradiation processes were repeated. Nanoparticles were prepared by chemical precipitation route using zinc acetate, sodium hydroxide and absolute ethanol. Zinc acetate dehydrate (0.2195 g) was dissolved in 20 mL of absolute ethanol and stirred with a magnetic stirrer at room temperature, to be mixed thoroughly. Then the solution of NaOH (0.08 g NaOH in 20 mL of absolute ethanol) was added drop-wise into the solution of zinc acetate under constant magnetic stirring for 1 h. After that, 0.015 mmol of oleic acid was added into the solution. The white powder was obtained after stirring this solution at room temperature for another 1 h. The prepared dispersion was centrifugally filtered and washed several times with ethanol and distilled water, then dried in an oven at 50 °C for 4 h.[17]

3.1.3. Characterization of NPs

The properties of the prepared nanoparticles were found with the help of a scanning electron microscope (SEM) and X-ray diffraction (XRD).

3.1.4. Dosimetry with NPs

At the next stage, various concentrations of ZnO NPs (500, 1000, 3000 μg ml-1) were incorporated into the composition of PRESAGE and the irradiation processes were repeated in three small fields (1×1, 2×2 and $3 \times 3 cm^2$).

Ultimately, by comparing the results of optical density changes in the presence and absence of NPs, dose enhancement factor was determined.

3.2. Monte Carlo simulation

MCNP5 Monte Carlo code was used to simulate the related geometry. At the onset of this part, by using information of Varian oncology system, the head of Varian Clinac 2100C linear accelerator, producing 6 MV photon beams, consisting of a target, primary collimator, flattening filter, ion chamber, secondary collimator, and a water phantom with dimensions of $30 \times 30 \times 30 cm^3$ at distance of 100 cm from the target were simulated. The number of particles was set to be 2×10^9 and the *f8 tally was used to calculate energy deposition of electrons, photons and neutrons at specific points.

The extracted parameters of this simulation were percentage depth dose (PDD) and beam profile of 6 MV photon beams in a $3 \times 3 cm^2$ field size.

In order to validate the simulation, a relative dosimetry was done in a water phantom and mentioned field size. Then, the obtained PDD and beam profile were compared with those of simulation. Since there is a high dose gradient in small radiation fields, in order to create a better spatial resolution of the measured data, the smallest effective volume of the ion chamber (0.015 cc), known as pinpoint (PTW, Freiburg, Germany), was used.

The next step was the simulation of ZnO NPs and PRESAGE dosimeter. PRESAGE compositions, which are shown in Table 1, were simulated with dimension of $1 \times 1 \times 3.5 cm^3$, located in the water phantom.

For NPs simulation, initially the required concentration of nanoparticles was specified. Then, the number of nanoparticles in a certain concentration was calculated. This procedure is as follows:

If 500 $\mu g\, ml^{-1}$ of ZnO NPs was incorporated into a volume of $3.5 cm^3$ water equivalent PRESAGE composition, the volume of applied NPs would be $3.1 \times 10^{-4} cm^3$.

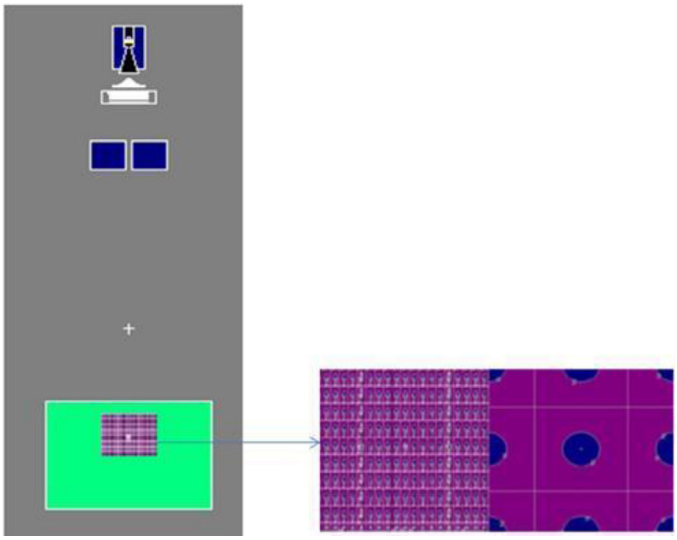

Fig. 2. Schematic of simulated geometry and NPs distributions.

On the other hand, the volume of each sphere of NPs is calculated by Eq. (1).

$$v = \frac{4}{3}\pi r^3 \quad (1)$$

Where v and r represent the volume and radius of the sphere, respectively. By using scanning electron microscopy (SEM), the average diameter of nanoparticles was determined to be about 40 nm. Therefore, the volume of each nanoparticle would be 3.3×10^{-17} cm^3. By dividing the total volume by that of each nanoparticle, the number of NPs was established as 9×10^{12}.

By repeating lattices in such a way to locate one NP in each cell, the uniform distribution of NPs was simulated.

In order to get this pattern, three levels of lattice definitions were used. The sizes of these levels were in orders of millimeter, micrometer and nanometer, respectively. Millimeter and micrometer cubic cells were filled by PRESAGE substance and the nanometer cells contained nanoparticles. In order to reduce runtime for further process, phase space file was used. This option of the MCNP5 code is one of the variance reduction methods that makes it possible to simulate a radiation source in an input and hypothetically see the influence of that source in another input file. Since low energy photon beams and electrons have significant influence on DEF, no energy cut off was used and by using the *f8 tally, the deposited energy was acquired across the central axis and at depth of maximum dose (2.5 cm) in terms of MeV and, then, DEF was obtained as the ratio of deposited energy in the presence of NPs to that of a no NPs condition. Fig. 2 depicts the schematic of simulated geometry and NPs distributions.

Finally the results of the calculated and measured DEF were compared.

4. Results

4.1. PRESAGE dosimetry

The XRD pattern of synthesized ZnO nanoparticles is shown in Fig. 3. X-ray diffraction study confirmed that the synthesized materials were ZnO and all the diffraction peaks agreed with the reported JCPDS data. By using EM3200 Scanning Electron Microscopy (KYKY, Ontario, USA), the size distribution of Zinc Oxide NPs was determined. As can be seen in Fig. 4, the mean size of NPs is about 40 nm.

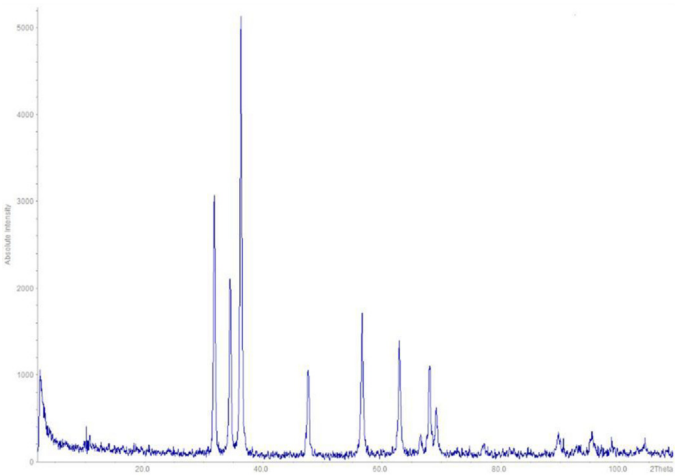

Fig. 3. XRD pattern of prepared ZnO NPs.

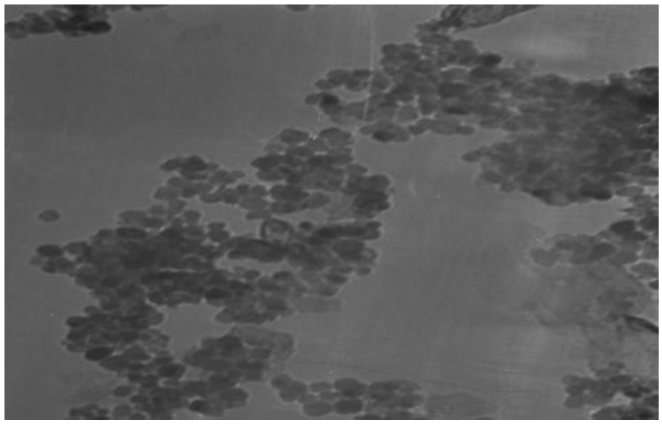

Fig. 4. SEM photo of ZnO NPs.

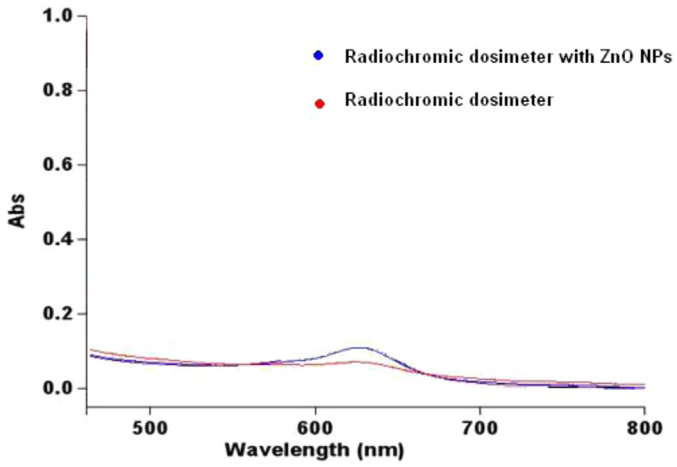

Fig. 5. The absorption spectrum of PRESAGE with and without NPs over visible wavelengths.

Fig. 5 represents the absorption spectrum of PRESAGE with and without NPs over visible wavelength. As can be seen, the maximum absorption of samples occurred at about 632 nm.

Fig. 6 depicts the calibration curve of PRESAGE over various dose levels. This calibration is determined at a wavelength of 632 nm which was the maximum absorption wavelength of PRESAGE.

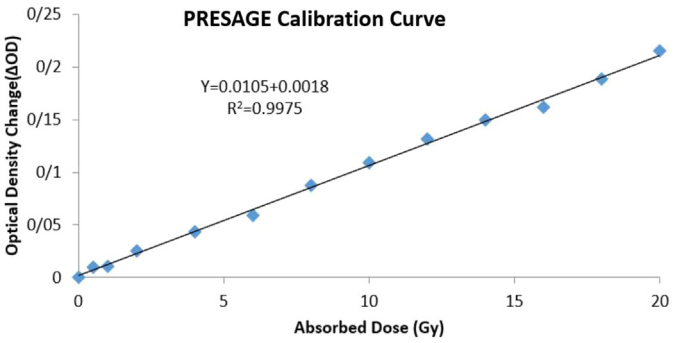

Fig. 6. PRESAGE calibration curve.

Table 2
DEF measured by PRESAGE.

DEF	Concentration of NPs	Field size (cm^2)
1.361.391.44	500 μg/mL1000 μg/mL3000 μg/mL	1*1
1.391.411.46	500 μg/mL1000 μg/mL3000 μg/mL	2*2
1.401.451.50	500 μg/mL1000 μg/mL3000 μg/mL	3*3

Dose enhancement factor (DEF) is defined as the ratio of changes in optical density with NPs to the optical density changes without NPs.[18]

Since PRESAGE exhibits a linear behavior against various dose levels (Fig. 6), by comparing the optical density changes at a particular dose step with and without NPs, DEF could be determined.

The DEF, as defined above, was then acquired for different compositions of PRESAGE in the small studied fields (Table 2).

4.2. Monte Carlo simulation

Fig. 7 shows the percentage depth dose and beam profile of the $3 \times 3\,cm^2$ field irradiated by 6 MV photon beams, obtained by MCNP5 code and pinpoint ion chamber as the simulation validation parameters.

Table 3 shows the comparison of acquired data by simulation and ion chamber. A good agreement (around 2% deviation) is found between experimental measurement and simulation data. Therefore, the results of simulation are reliable.

Table 4 shows the DEF obtained by simulation. Fig. 8 delineates the comparison of data obtained by experimental measurements and Monte Carlo simulation for various concentrations of applied NPs in three studied field sizes. This figure implies that the results obtained by simulation are not consistent with experimental data. Moreover, a small increscent in DEF is shown by increasing the concentrations of NPs and field sizes.

Since in small radiation fields, lateral electronic equilibrium does not exist, higher numbers of monitor units (MU) are needed to deliver a certain amount of absorbed dose.[19]

Higher amounts of MU lead to excessive time of treatment and, consequently, the probability of random errors and patient movements during treatment will rise. Therefore, finding a solution to overcome such a problem is essential. The results of this study showed that a good value of DEF could be derived by incorporating ZnO NPs.

Experimental measurements and simulation data (Fig. 8) show that dose enhancement grows by increasing the concentration of NPs. In fact, by increasing the concentration of NPs, the number of NPs in a certain volume of PRESAGE would increase and, therefore, the probability of photon interaction with NPs would increase

Table 3
Variation of validation parameters obtained by MCNP5 and ion chamber.

	Parameter	Ion Chamber	Monte Carlo	Difference
Percentage Depth Dose	Max difference at build up region (%)			2.2%
	R50(cm)	12.8	13.1	
	R80(cm)	5.5	5.9	
	R90(cm)	3.5	3.6	
	Max dose point (cm)	1.6	1.8	
Beam Profile	Max difference at flat region (%)			0.9%
	Max difference at penumbra region (%)			0.4%
	FWHM	3	2.97	

Table 4
DEF calculated bsy Monte Carlo simulation.

DEF	Concentration of NPs	Field size (cm^2)
1.051.081.10	500 μg/mL1000 μg/mL3000 μg/mL	1*1
1.061.091.10	500 μg/mL1000 μg/mL3000 μg/mL	2*2
1.081.111.13	500 μg/mL1000 μg/mL3000 μg/mL	3*3

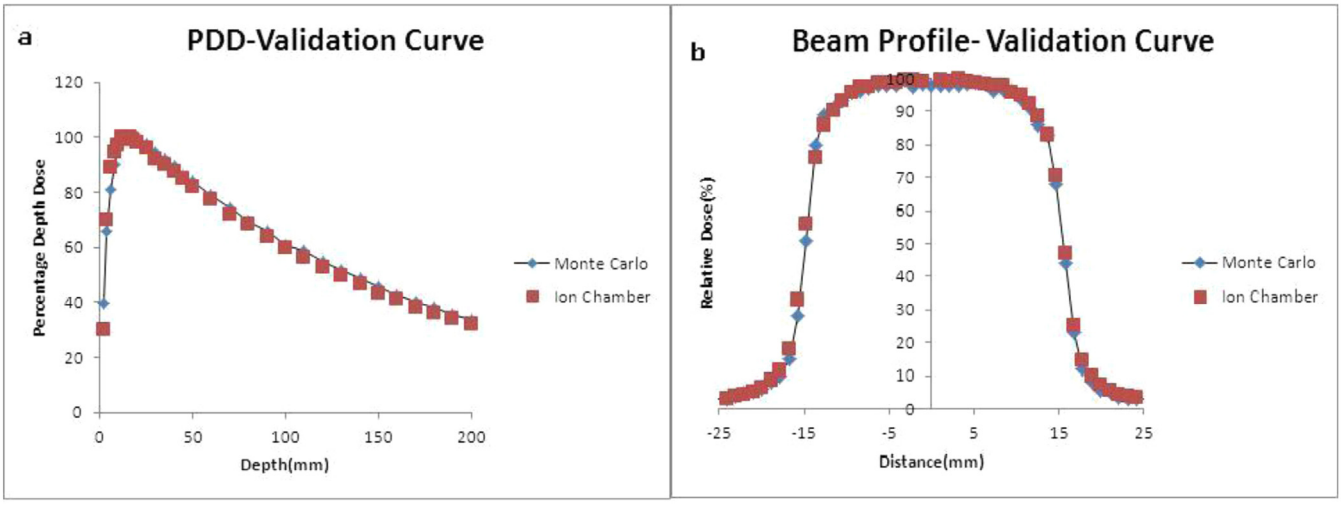

Fig. 7. Monte Carlo validation parameters. a: Percentage depth dose obtained by MCNP5 and pinpoint ion chamber. b: Beam profile obtained by MCNP5 and pinpoint ion chamber.

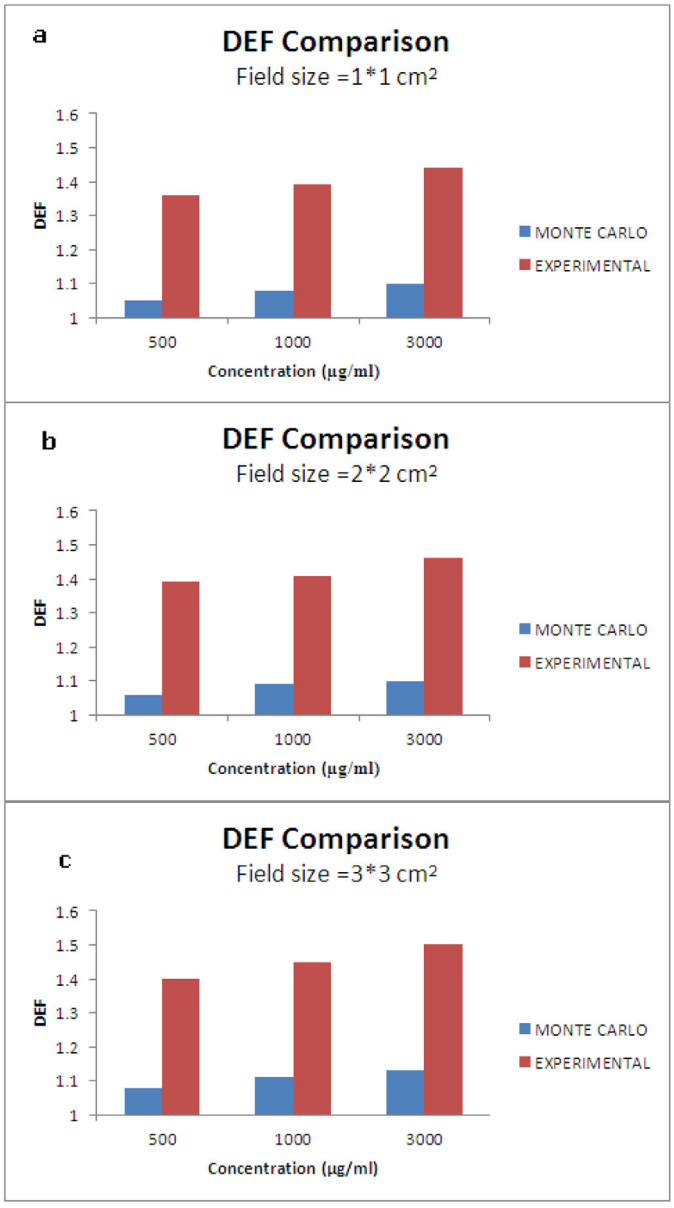

Fig. 8. DEF comparison for various field sizes and NPs' concentration. a: 1 × 1 field size, b: 2 × 2 field size, c:3 × 3 field size.

and, hence, the DEF would grow and consequently the needed MU to deliver each step of absorbed dose would reduce. But it should be noted that the correlation between increasing dose enhancement and concentration of NPs is not linear. As shown in Fig. 8, two fold increase in concentration of NPs leads to a little growth of DEF. The explanation for this matter is probably that the increase in concentration of NPs shields the radiosensitive components of the dosimeter (LMG) interacting with X-rays. In other words, radiation interacts with the NPs and produces secondary electrons and free radicals or ions. These products should interact directly with the LMG converting it to its oxidized form. However, increasing the concentration of NPS could show a shielding property, preventing the electrons hit the LMG.[20]

As Tables 2 and 4 illustrate, DEF increases by increasing field size. That reveals that by decreasing the size of radiation field, lateral scatter disequilibrium becomes higher which causes less output factor for such fields compared to bigger ones.

In order to reach logic DEF, homogeneous dispersion of NPs in the irradiated volume is needed. Regarding the heavy weight of ZnO NPs compared to PRESAGE, some portion of this substance may be settled in PRESAGE. Whereas, in the simulation section, the distribution of NPs in PRESAGE structure is completely homogeneous. In order to create a similar condition of simulation and experimental measurements and prevent the settling of NPs, as explained in NPs synthesization section, Oleic acid was added to the composition of the needed materials. This substance makes the NPs dispersible in organic solvents and to some extent reduces their aggregation.[17]

The other important parameter in calculating and measuring DEF is the method of selecting sampling points. In other words, the energy deposition in the Monte Carlo section is calculated in the introduced cells with certain dimensions and also positions. Readout by UV-Vis spectrophotometer is done on the whole thickness of the cuvettes. Therefore, the data extracting points in Monte Carlo simulation and UV-Vis spectrophotometer do not quite match. It is also notable that the size distribution of NPs may have an important role on DEF. As shown in Fig. 3, in reality, sizes of NPs are not definite and have a spectrum. However, in the Monte Carlo section, the mean size of NPs was used to do the simulation.

Furthermore, as explained in methodology, in order to take into consideration the effects of the low energy electrons on dose enhancement factor, no energy cut off was used. By not specifying a cut off energy in the input file, MCNP5 uses a minimum cut off energy of 1 keV for both electrons and photons.[21] In this way, a large number of Auger electrons whose energy is below the cut off would be ignored. However, in reality, these electrons and photons still leak out of the NP and contribute to the dose outside of the NP. Therefore, it seems that MCNP5 is not the best tool to compute the energy deposition of such low energy electrons.

Therefore, the differences in results of the DEF obtained by experimental measurements and simulation could be the consequences of various patterns of NPs' distribution, different style of data extracting points, not considering the size distribution of NPs in simulation and also the effects of Auger electrons which are ignored in simulation.

Although DEF is usually attributed by Orthovoltage photon beams, where photoelectric effect is dominant, the results of this study showed that DEF can be achieved by megavoltage photon beams as well. In this situation, DEF may be the results of low energy photons in the continuous X-ray spectrum, attenuated photons, probably the pair production effect and even Compton scattering. By incorporating ZnO NPs into PRESAGE structure, the electrical density of the irradiated volume would increase and therefore the cross section of Compton scattering and probability of producing secondary electrons or free radicals which have significant effect on DEF would increase.[1]

The results of this study are consistent with previous studies and the slight differences might be the effect of size and concentration of nanoparticles.[22–23]

5. Conclusion

The results of this study showed that ZnO NPs could be used as dose enhancing substances for megavoltage irradiation condition. Experimental measurements and simulation data showed that dose enhancement increased by increasing concentration of NPs and, therefore, the therapeutic ratio would grow. Many reasons such as photoelectric, pair production effects and even Compton scattering can cause DEF. Although MCNP5 simulation code can be considered as a proper method for simulating NPs distribution, the weak potential of MCNP5 in tracing the Auger electrons cause the energy deposition of such low energy particles to be underestimated.

Conflict of interest

None.

Financial disclosure

None.

References

1. Townley HE, Rapa E, Wakefield G, Dobson PJ. Nanoparticle augmented radiation treatment decreases cancer cell proliferation. *Nanomedicine*. 2012;8:526–536.
2. Schilling K, Bradford B, Castelli D, et al. Human safety review of ñanoẗitanium dioxide and zinc oxide. *Photochem Photobiol Sci*. 2010;9:495–509.
3. Liong M, Lu J, Kovochich M, et al. Multifunctional inorganic nanoparticles for imaging, targeting, and drug delivery. *ACS Nano*. 2008;2:889–896.
4. Li XH, Xing YG, Li WL, Jiang YH, Ding YL. Antibacterial and physical properties of poly (vinyl chloride)-based film coated with ZnO nanoparticles. *Food SciTechnolInt*. 2010;163:225–232.
5. Moos PJ, Chung K, Woessner D, Honeggar M, Cutler NS, Veranth JM. ZnO particulate matter requires cell contact for toxicity in human colon cancer cells. *Chem Res Toxicol*. 2010;23:733–739.
6. Franklin NM, Rogers NJ, Apte SC, Batley GE, Gadd GE, Casey PS. Comparative toxicity of nanoparticulateZnO, bulk ZnO, and ZnCl2 to a freshwater microalga (Pseudokirchneriellasubcapitata): The importance of particle solubility. *Environ Sci Technol*. 2007;41:8484–8490.
7. Mills A, Lee SK. A web-based overview of semiconductor photochemistry-based current commercial applications. *J Photochem Photobiol A: Chem*. 2002;152:233–247.
8. Sharma V, Anderson D, Dhawan A. Zinc oxide nanoparticles induce oxidative DNA damage and ROS-triggered mitochondria mediated apoptosis in human liver cells (HepG2). *Apoptosis*. 2012;17:852–870.
9. Hanley C, Thurber A, Hanna C, Punnoose A, Zhang J, Wingett DG. The influences of cell type and ZnO nanoparticle size on immune cell cytotoxicity and cytokine induction. *Nanoscale Res Lett*. 2009;4:1409–1420.
10. Tamura K, Ohko Y, Kawamura H, et al. X-ray induced photoelectrochemistry on TiO_2. *Electrochim Acta*. 2007;52:6938–6942.
11. Turner JA. *Atoms, radiation, and radiation protection*. New York: John Wiley & Sons, Inc.; 1995.
12. Dasa JI, Ding GX, Ahnesjö A. Small fields: Nonequilibrium radiation dosimetry. *Med Phys*. 2008;35:206–215.
13. Khezerloo D, Nedaie HA, Takavar A, et al. PRESAGE® as a solid 3-D radiation dosimeter: A review article. *Radiat Phys Chem*. 2017;141:88–97.
14. Cho SH, Jones BL, Krishnan ST. Hedosimetric feasibility of gold nanoparticle-aided radiation therapy (GNRT) via brachytherapy using low-energy gamma-/x-ray sources. *Phys Med Biol*. 2009;54:4889–4905.
15. Taha E, Djouider F, Banoqitah E. Monte Carlo simulation of dose enhancement due to silver nanoparticles implantation in brain tumor brachytherapy using a digital phantom. *Radiat Phys Chem*. 2019;156:15–21.
16. Khan FM. *The physics of radiation therapy*. Philadelphia: Lippincott Williams & Wilkins; 2010.
17. Rouhipour Mikal N, Sadjadi S, Rajabi-Hamane M, Ahmadi SJ, Iravani E. Decoration of electrospunpolyacrylonitrilenanofibers with ZnO nanoparticles and their application for removal of Pb ions from waste water. *J IRAN CHEM SOC*. 2016;13:763–771.
18. Mousavie Anijdan SH, Shirazi A, Mahdavi SR, et al. Megavoltage Dose enhancement of gold nanoparticles for different geometric set-ups: Measurements and Monte Carlo simulation. *Iran. J. Radiat. Res*. 2012;10:183–186.
19. Bagheri Hamed, Soleimani Azadeh, Gharehaghaji Nahideh, et al. An overview on small-field dosimetry in photon beam radiotherapy: Developments and challenges. *J Cancer Res Ther*. 2017;13:175–185.
20. Khadem-Abolfazli M, Mahdavi M, Mahdavi SRM, Ataei Dr Gh. Dose enhancement effect of gold nanoparticles on MAGICA polymer gel in mega voltage radiation therapy. *Int J Radiat Res*. 2013;11(1):55–61.
21. X-5 Monte Carlo Team, MCNP — A General Monte CarloN-Particle Transport Code, Version 5., Los Alamos National Laborator, April 24, 2003.
22. Zangeneh Masoumeh, Nedaei Hassan Ali, Mozdarani Hossein, Mahmoudzadeh Aziz, Kharrazi Sharmin, Salimi Mahdieh. The role and mechanisms of zinc oxide nanoparticles in the improvement of the radiosensitivity of lung cancer cells in clinically relevant megavoltage radiation energies in-vitro. *Nanomed J*. 2019;6:85–99.
23. Banaee N, Nedaie HA, Shirazi AR, Zirak AR, Sadjadi S. Evaluating the effect of Zinc Oxide nanoparticles doped with Gadolinium on dose enhancement factor by PRESAGE dosimeter. *Int J Radiat Res*. 2016;14(2):119–125.